

Drastic facilitation of the onset of global chaos in a periodically driven Hamiltonian system due to an extremum in the dependence of eigenfrequency on energy

S.M. Soskin^{1,2}, O.M. Yevtushenko³, and R. Mannella^{2,4}

¹*Institute of Semiconductor Physics, National Academy of Sciences of Ukraine, Kiev, Ukraine*

²*Department of Physics, Lancaster University, Lancaster LA1 4YB, UK*

³*ICTP, Trieste, Italy*

⁴*Dipartimento di Fisica, Università di Pisa and INFN UdR Pisa, 56100 Pisa, Italy*

(November 13, 2018)

The Chirikov resonance-overlap criterion predicts the onset of global chaos if nonlinear resonances overlap in energy, which is conventionally assumed to require a non-small magnitude of perturbation. We show that, for a time-periodic perturbation, the onset of global chaos may occur at unusually *small* magnitudes of perturbation if the unperturbed system possesses more than one separatrix. The relevant scenario is the combination of the overlap in the phase space between resonances of the same order and their overlap in energy with chaotic layers associated with separatrices of the unperturbed system. One of the most important manifestations of this effect is a drastic increase of the energy range involved into the unbounded chaotic transport in spatially periodic system driven by a rather *weak* time-periodic force, provided the driving frequency approaches the extremal eigenfrequency or its harmonics. We develop the asymptotic theory and verify it in simulations.

05.45.Ac, 05.45.Pq, 75.70.cn

A weak perturbation of a Hamiltonian system causes the onset of chaotic layers in the phase space around separatrices of the unperturbed system and/or separatrices surrounding nonlinear resonances generated by the perturbation itself [1–3]: the system may be transported along the layer random-like. Chaotic transport plays an important role in many physical phenomena [3]. If the perturbation is weak enough, then the layers are thin and such chaos is called *local* [1–3]. As the magnitude of the perturbation increases, the widths of the layers grow and the layers corresponding to adjacent separatrices (either to those of the unperturbed system, or to separatrices surrounding different nonlinear resonances) reconnect at some, typically non-small, critical value of the magnitude, which conventionally marks the onset of *global* chaos [1–3] i.e. chaos in a large range of the phase space which increases with a further increase of the magnitude of perturbation. Such scenario often correlates with the overlap in *energy* between neighbouring resonances calculated *independently* in the resonant approximations of the corresponding orders: this constitutes the celebrated empirical Chirikov resonance-overlap criterion [1–3].

But the Chirikov criterion may fail in time-periodically perturbed *zero-dispersion* (ZD) systems [4–6] (cf. also studies of related maps [7,8]) i.e. systems in which the frequency of eigenoscillation possesses an extremum (typically, a local maximum or minimum) as a function of its energy. In such systems, there are typically two resonances of one and the same order [9], and their overlap in energy does not result in the onset of global chaos [5–8]. Even their overlap in phase space results typically, instead of the onset of global chaos, only in reconnection of the thin chaotic layers associated with the resonances while, as the amplitude of the time-periodic perturbation grows further, the layers *separate* again (with a different

topology [5–8]) despite the *growth* of the width of the overall relevant range of energy.

The major idea of the *present* work is to *limit* the energy range relevant to the overlap of resonances of the same order by chaotic layers relating either to resonances of a different order [10] or to separatrices of the unperturbed system (these scenarios immediately suggest the corresponding substitute for the Chirikov criterion in a ZD system in the range of extremum). The onset of global chaos occurs respectively in a broader energy range or at *unusually small* magnitudes of the perturbation. The former case will be considered elsewhere while we present below details of the latter case. It relates to many important systems and the above effect is manifested in a very strong manner: *all* systems with more than one separatrices possess the ZD property [5,6] and global chaos may involve the whole energy range between the separatrices.

We use as an example a potential system with a periodic potential possessing two different-height barriers in a period (Fig. 1(a)):

$$H_0(p, q) = \frac{p^2}{2} + U(q), \quad U(q) = \frac{(\Phi - \sin(q))^2}{2}, \quad (1)$$

$$\Phi = \text{const} < 1.$$

The model (1) may describe e.g. a 2D electron gas in a magnetic field spatially periodic in one of dimensions of the gas [11]. The interest to this system arose due to technological advances of the last decade allowing to manufacture high-quality magnetic superlattices [12,13] leading to a variety of interesting behaviours of charge carriers in semiconductors (see [11–15] and references therein). The same model describes a pendulum on a hinge spinning about its vertical axis [16].

The separatrices of the Hamiltonian system (1) in the $p - q$ plane and the dependence of the frequency ω of its oscillation, often called *eigenfrequency*, on energy $E \equiv H_0(p, q)$ are shown in Figs. 1(b) and 1(c) respectively. As seen from the latter, $\omega(E)$ is close to the extreme eigenfrequency $\omega_m \equiv \omega(E_m)$ in the major part of the interval $[E_b^{(1)}, E_b^{(2)}]$ while sharply decreasing to zero as E approaches $E_b^{(1)}$ or $E_b^{(2)}$. Such features of $\omega(E)$ are *typical* for systems with two or more separatrices.

Let the time-periodic perturbation be added:

$$\begin{aligned} \dot{q} &= \partial H / \partial p, & \dot{p} &= -\partial H / \partial q, \\ H(p, q) &= H_0(p, q) - hq \cos(\omega_f t). \end{aligned} \quad (2)$$

Let us first consider the *conventional* evolution of chaos in the system (2)-(1) as h grows while ω_f remains fixed at an arbitrarily chosen value beyond the immediate vicinity of ω_m and its harmonics. It is illustrated by Fig. 2. At small h , there are two thin chaotic layers, around the inner and outer separatrices of the unperturbed system. Unbounded chaotic transport takes place only in the outer chaotic layer i.e. in a *narrow* energy range. As h grows, so also do the layers until, at some critical value $h_{gc} \equiv h_{gc}(\omega_f)$, they merge. This event may be considered as the onset of global chaos: the whole range of energies between the barriers levels then becomes involved in unbounded chaotic transport. Note that the states $\{I^{(l)}\} \equiv \{p = 0, q = \pi/2 + 2\pi l\}$ and $\{O^{(l)}\} \equiv \{p = 0, q = -\pi/2 + 2\pi l\}$ (where $l = 0, \pm 1, \pm 2, \dots$) in the stroboscopic (for instants $n2\pi/\omega_f$ with $n = 0, 1, 2, \dots$) Poincaré section are associated respectively with the inner and outer saddles of the unperturbed system, and necessarily belong to the inner and outer chaotic layers respectively. Thus, the necessary and sufficient condition for global chaos to arise in the system may be formulated as the possibility for the system placed initially in the state $\{I^{(0)}\}$ to pass beyond the neighbouring ‘‘outer’’ states, $\{O^{(0)}\}$ and $\{O^{(1)}\}$, i.e. for $q(t \gg 2\pi/\omega_f)$ to become smaller than $-\pi/2$ or larger than $3\pi/2$.

A diagram in the $h - \omega_f$ plane, based on the above criterion, is shown in Fig. 3. The lower boundary of the shaded area represents the function $h_{gc}(\omega_f)$. It has deep cusp-like local minima (*spikes*) at frequencies $\omega_f = \omega_s^{(n)}$ that are slightly less than the odd multiples of ω_m ,

$$\omega_s^{(n)} \approx \omega_m(2n - 1), \quad n = 1, 2, \dots \quad (3)$$

The deepest minimum occurs at $\omega_s^{(1)} \approx \omega_m$: $h_{gc}(\omega_s^{(1)})$ is approximately 40 times smaller than in the neighbouring pronounced local maximum of $h_{gc}(\omega_f)$ at $\omega_f \approx 1$. As n increases, an n th minimum becomes less deep.

The origin of the spikes becomes obvious from the analysis of the evolution of the Poincaré section as h grows while $\omega_f \approx \omega_s^{(1)}$. For $h = 0.001$, one can see in Fig. 4(a) four chaotic trajectories: those associated with

the inner and outer separatrices of the unperturbed system [1–3] are coloured green and blue respectively, while the trajectories associated with the two nonlinear resonances of the 1st order [1–3] are indicated by red and cyan (the corresponding attractors are indicated respectively by crosses of the same colours). Examples of non-chaotic (often called KAM [1–3]) trajectories separating the chaotic ones are shown in brown. As h increases to $h = 0.003$ (Fig. 4(b)), the blue and red chaotic trajectories mix: the resulting chaotic layer is shown in blue. As h increases further (see Fig. 4(c), where $h = 0.00475$), the latter layer merges with the layer associated with the cyan chaotic trajectory (the resulting layer is shown by blue) and, finally, as h increases slightly more (see Fig. 4(d), where $h = 0.0055$), the latter layer merges with the layer associated with the green trajectory [17], thereby marking the onset of global chaos as defined above.

For most of the range $[E_b^{(1)}, E_b^{(2)}]$, $\omega(E)$ is close to ω_m [18] (cf. Fig. 1(c)), so that the overlap between the resonances of the *same* order may be described within the resonance approximation. Given that it plays the main role in the above scenario, the function $h_{gc}(\omega_f)$ may also be evaluated in the ranges of the spikes using the resonance approximation. The explicit asymptotic (for $\Phi \rightarrow 0$) formulae for the minima themselves, in the lowest order of the parameters of smallness, are as follows:

$$\begin{aligned} \omega_s^{(n)} &= \frac{(2n - 1)\pi}{2 \ln(4e/\Phi)}, \quad n = 1, 2, \dots, \\ \Phi^2 &\ll 1, \quad \{10 \ln(4e/\Phi)\}^{-1} \ll 1 \end{aligned} \quad (4)$$

(note that $\omega_m \approx \pi/\{2 \ln(8/\Phi)\}$, so that (4) does not contradict (3)),

$$\begin{aligned} h_{gc}(\omega_s^{(n)}) &= \frac{(2n - 1)c\Phi}{2\sqrt{2} \ln(4e/\Phi)}, \quad c \approx 0.179, \quad n = 1, 2, \dots, \\ \Phi^2 &\ll 1, \quad \frac{2n - 1}{\ln(4e/\Phi)} \ll 1, \\ \frac{\ln\{10 \ln(4e/\Phi)/(2n - 1)\}}{10 \ln(4e/\Phi)/(2n - 1)} &\ll 1, \end{aligned} \quad (5)$$

where c is the root of the equation

$$\ln\left(\frac{1 + \chi(c)}{1 - \chi(c)}\right) - 2\chi(c) = c, \quad \chi(c) \equiv \sqrt{1 - 4e^{c-2}}. \quad (6)$$

Eqs. (4)-(6) have been derived within the following self-contained scheme. Let ω_f be close to $n\omega_m$ so that, for most of the energy interval $[E_b^{(1)}, E_b^{(2)}]$ except in the close vicinity of barriers levels, the n th harmonic of eigenoscillation is nearly resonant to the driving. Then a slow dynamics of action I and angle ψ [19] may be described by the following auxiliary Hamiltonian (cf. [1–8]):

$$\tilde{H}(I, \psi) = \int_{I(E_m)}^I dI (n\omega - \omega_f) - nhq_n \cos(\tilde{\psi}), \quad (7)$$

where $I \equiv I(E) = (2\pi)^{-1} \oint dq p$ is action (note also that $dE/dI = \omega$ [19]) and $\tilde{\psi} \equiv n\psi - \omega_f t$ is slow angle [1–8] while $q_n \equiv q_n(I)$ is the modulus of the n th Fourier harmonic of coordinate (see the exact definition in [5,6]).

For a given value of h and ω_f , there are typically two stable stationary points in a 2π band of the $I - \tilde{\psi}$ plane, often called *resonances* of the n th order. Each resonance is surrounded by a *separatrix* which includes one (per a 2π band) unstable stationary point, called saddle. If both saddles possess the same \tilde{H} the separatrices reconnect each other. This condition is satisfied along some line $\omega_f(h)$ in the $h - \omega_f$ plane. We need to find the point (ω_s, h_s) on this line such that the lowest along the reconnected separatrices energy E_l coincides with the upper energy boundary $E_{cl}^{(1)}$ of the chaotic layer around the lower barrier level $E_b^{(1)}$ (one can prove that the chaotic layer around the upper barrier level is then necessarily overlapped by the resonance separatrices: cf. Fig. 4(c)). It is known [3] that, if $\omega_f \lesssim \omega_0$ where ω_0 is the eigenfrequency at the bottom of the wells, then $\delta \equiv E_{cl}^{(1)} - E_b^{(1)} \sim h\omega_f/\omega_0$. One can prove that, if $\Phi \rightarrow 0$, then the values of ω_s and h_s are not sensitive to the exact value of δ within this range. Thus, the values of ω_s and h_s can be obtained using only the *resonant approximation*.

In the unperturbed case ($h = 0$), the equations of motion (2)-(1) can be solved explicitly, and $\omega(E)$ can be found then explicitly too. As $\Phi \rightarrow 0$, it reduces to

$$\omega(E) = \frac{\pi}{\ln\left(\frac{64}{(\Phi - \Delta E)(\Phi + \Delta E)}\right)}, \quad \Delta E \equiv E - \frac{1}{2}, \quad (8)$$

$$\Phi \ll 1.$$

Substituting Eq. (8) for ω into Eq. (7) for \tilde{H} and assuming that $q_{2n-1} \xrightarrow{\Phi \rightarrow 0} \sqrt{2}/(2n-1)$ in the relevant energy range (note that $q_{2n} = 0$ due to the symmetry of the potential), one can derive Eqs. (4)-(6) as the solution of the system of two algebraic equations obtained from the condition of the equality of \tilde{H} in the saddles and from the condition that $E_l - E_b^{(1)} \sim h\omega_f/\omega_0$, keeping in the solution only those terms which have the lowest order in the parameters of smallness. The solution confirms the original assumptions that $\omega \approx \omega_f/(2n-1)$ and $q_{2n-1} \approx \sqrt{2}/(2n-1)$ in the relevant range of energies, which proves that the theory is self-contained. Note also that, to logarithmic accuracy, the asymptotic formulas (4)-(6) are valid for an arbitrary symmetric potential (whose period is normalized to 2π) and they may be rather easily generalized for an *arbitrary* Hamiltonian system with two separatrices close to each other.

The values of $\omega_s^{(n)}$ obtained from simulations for $\Phi = 0.2$ (see Fig. 3) nicely agree with Eq. (4). As concerns $h_{gc}(\omega_s^{(n)})$, the value $\Phi = 0.2$ is too large for Eq. (5) to be accurate but, even so, Eq. (5) provides a very good estimate for $h_{gc}(\omega_s^{(1)})$ and the correct order of magnitude

for $h_{gc}(\omega_s^{(2)})$ (see Fig. 3). Calculations within the same scheme but using exact formulas for ω and q_{2n-1} and solving the system of the algebraic equations numerically yield the values $(\omega_s^{(1)} = 0.4 \pm 0.004, h_{gc}(\omega_s^{(1)}) = 0.005 \pm 0.001)$ and $(\omega_s^{(2)} = 1.243 \pm 0.01, h_{gc}(\omega_s^{(2)}) = 0.025 \pm 0.008)$, nicely agreeing with the simulations.

It is worth mentioning two generalizations:

1. For *non-symmetric* $U(q)$, $q_{2n} \neq 0$ and, therefore, pronounced spikes in $h_{gc}(\omega_f)$ exist at $\omega_f \approx 2n\omega_m$ too.

2. If the time-periodic driving is *multiplicative*, then the resonances become *parametric* (cf. [19]). Parametric resonances are more complicated and much less studied than nonlinear resonance. But, still, the main mechanism for the onset of global chaos remains the same, and simulations show that $h_{gc}(\omega_f)$ do possess deep spikes. At the same time, the frequencies of the main spikes are twice as large as those of the corresponding spikes in the case of the additive driving: this is so because the characteristic frequencies of parametric resonance are typically doubled as compared with the nonlinear resonance (cf. [19]).

Finally, we suggest two examples of physical applications: (i) a jump-wise increase of the *dc conductivity* occurs due to the jump-wise increase of the range of energies involved in the unbounded chaotic transport of electric charge carriers in a magnetic superlattice (cf. [11]); (ii) a significant decrease of the *activation energy* for noise-induced multi-barrier escape in the presence of periodic driving is associated with the noise-free transport from the lower barrier to beyond the upper barrier (cf. [20,6]).

It is worth noting some analogies between our work and the work [21] describing the so called stochastic percolation in 2D Hamiltonian systems where the merging of internal and external chaotic zones was also relevant. However, both the models and the underlying mechanisms are very different (there is no zero-dispersion situation in [21]; rather the two-dimensionality is inherently important); besides, in [21], there was no explicit quantitative description analogous to our Eqs. (4)-(6).

The work was supported by INTAS Grants 97-574 and 00-00867. We are grateful to J. Howard, P. McClintock, J. Meiss and K. Richter for discussions.

-
- [1] B.V. Chirikov, Phys. Rep. **52**, 263 (1979).
 - [2] A.J. Lichtenberg, M.A. Liebermann, Regular and Stochastic Motion (Springer, New York, 1992).
 - [3] G.M. Zaslavsky, R.D. Sagdeev, D.A. Usikov and A.A. Chernikov, Weak Chaos and Quasi-Regular Patterns (Cambridge University Press, 1991).
 - [4] S.M. Soskin, Phys. Rev. E **50**, R44 (1994).
 - [5] S.M. Soskin et al., International Journal of Bifurcation and Chaos **7**, 923 (1997); R. Mannella, S.M. Soskin and P.V.E. McClintock, *ibid.* **8**, 701 (1998).

- [6] S.M. Soskin, R. Mannella, P.V.E. McClintock, Phys. Rep. **373**, 247 (2003).
- [7] J.E. Howard and S.M. Hohns, Phys. Rev. **A 29**, 418 (1984); D. del-Castillo-Negrete, J.M. Greene, P.J. Morrison, Physica **D 61**, 1 (1996); H. R. Dullin, J. D. Meiss, D. Sterling, Nonlinearity **13**, 203 (2000).
- [8] J.E. Howard and J. Humpherys, Physica **D 80**, 256 (1995).
- [9] More complicated cases are considered e.g. in [6,8].
- [10] If there are more than two resonances of the same order, then, for two given neighbouring same-order resonances, other resonances of the *same* order may sometimes play to some extent similar (i.e. limiting) role: cf. [8].
- [11] O.M. Yevtushenko and K.Richter, Phys. Rev. **B 57**, 14839 (1998); Physica **E 4**, 256 (1999).
- [12] H.A. Carmona et al., Phys. Rev. Lett. **74**, 3009 (1995).
- [13] P.D. Ye et al., Phys. Rev. Lett. **74**, 3013 (1995).
- [14] G.J.O. Schmidt, Phys. Rev. **B 47**, 13007 (1993).
- [15] P. Shmelcher, D.L. Shepelyansky, Phys. Rev. **B 49**, 7418 (1994).
- [16] A.A. Andronov, A.A. Vitt, S.E. Khaikin, Theory of Oscillators (Pergamon, Oxford, 1966).
- [17] We still use different colours for the trajectories starting from $\{I^{(0)}\}$ and $\{O^{(0)}\}$ in order to demonstrate that their mixing occurs very slowly, which indicates that the given \hbar is just slightly above the critical value \hbar_{gc} .
- [18] As $\Phi \rightarrow 0$, the $\omega(E)$ reduces to the rectangular form.
- [19] L.D. Landau and E.M. Lifshitz, Mechanics (Pergamon, London, 1976).
- [20] S.M. Soskin, R. Mannella, A.N. Silchenko, unpublished.
- [21] D.K. Chaikovsky, G.M. Zaslavsky, Chaos **1**, 463 (1991).

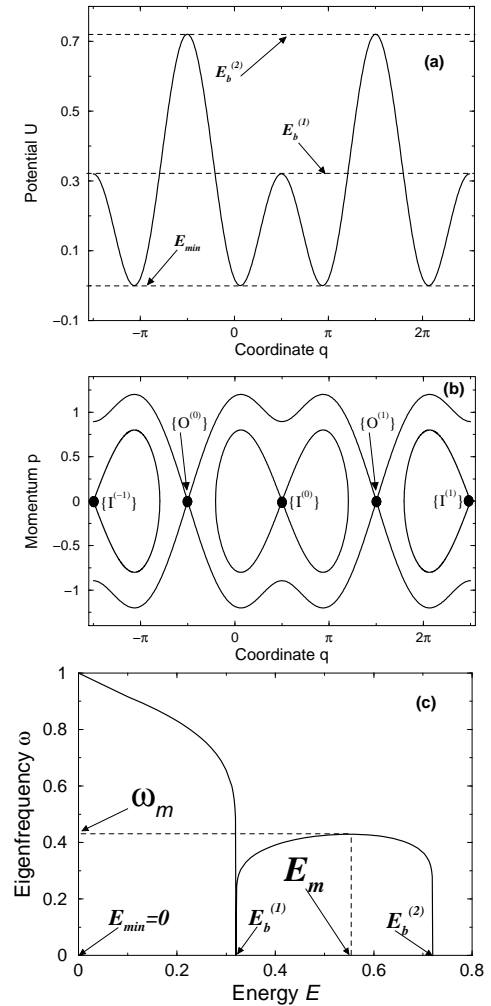


FIG. 1. The potential $U(q)$, the separatrices in the phase space and the eigenfrequency $\omega(E)$ for the unperturbed system (1) with $\Phi = 0.2$, in (a), (b) and (c) respectively.

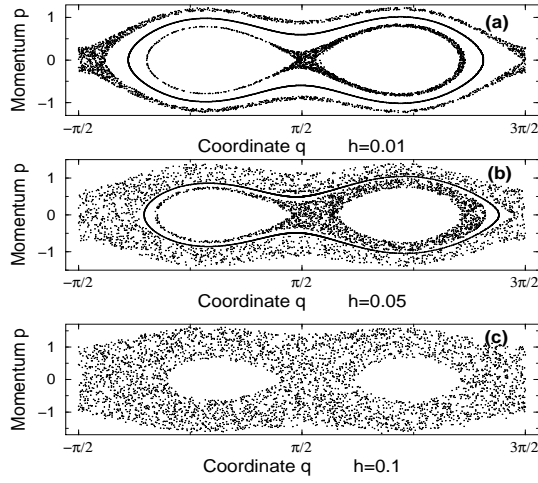


FIG. 2. The evolution of the stroboscopic (for instants $n2\pi/\omega_f$ with $n = 0, 1, 2, \dots$) Poincaré sections of the system (2)-(1) at $\Phi = 0.2$, with $\omega_f = 0.3$ while h grows from the top to the bottom: (a) 0.01, (b) 0.05, (c) 0.1. The number of points in each trajectory is 2000. In parts (a) and (b), three characteristic trajectories are shown: the inner trajectory starts from the state $\{I^{(0)}\} \equiv \{p = 0, q = \pi/2\}$ and is chaotic but bounded in the space; the outer trajectory starts from $\{O^{(0)}\} \equiv \{p = 0, q = -\pi/2\}$ and is chaotic and unbounded in coordinate; the third trajectory represents an example of a regular (KAM) trajectory separating the above chaotic ones. In (c), the chaotic trajectories mix.

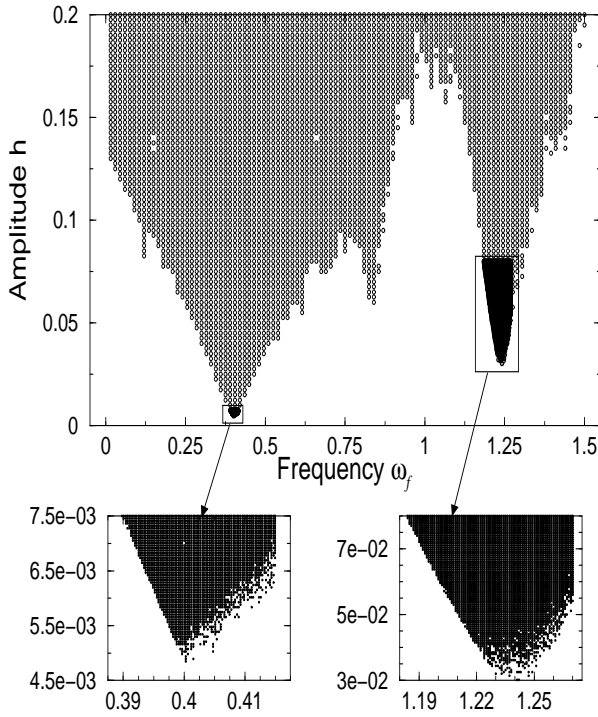


FIG. 3. The bifurcation diagram indicating (by shading) the perturbation parameters ranges at which global chaos exists. The integration time for each point of the grid is 12000π .

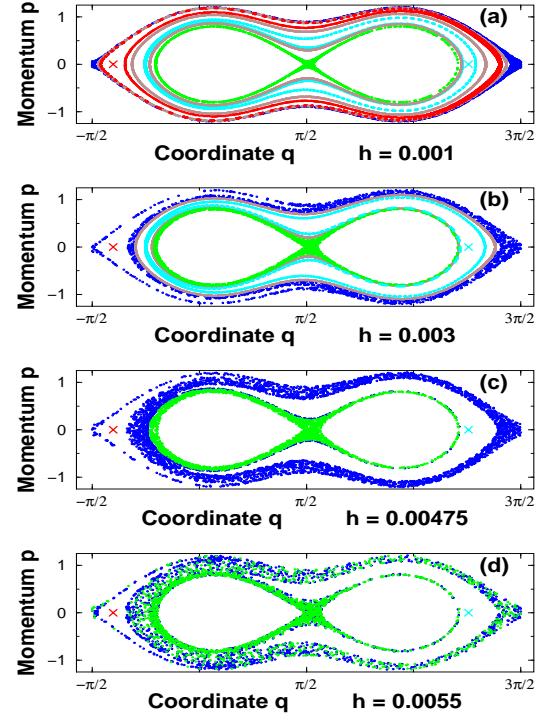


FIG. 4. The evolution of the stroboscopic Poincaré section of the system (2)-(1) with $\Phi = 0.2$ as the amplitude of the perturbation h grows while the frequency is fixed at $\omega_f = 0.401$. The number of points in each trajectory is 2000. The chaotic trajectories starting from the states $\{I^{(0)}\}$ and $\{O^{(0)}\}$ are drawn in green and blue respectively. The stable stationary points (the 1st-order nonlinear resonances) are indicated by the red and cyan crosses. The chaotic layers associated with the resonances, in those cases when they do not merge with those associated with the green/blue chaotic trajectories, are indicated in red and cyan respectively (their real width is much less than the width of the drawing line). Examples of KAM trajectories embracing the state $\{I^{(0)}\}$ while separating various chaotic trajectories are shown in brown.